Environmental Science & Technology

pubs.acs.org/est

Article

Projection of Mortality Burden Attributable to Nonoptimum Temperature with High Spatial Resolution in China

Published as part of Environmental Science & Technology virtual special issue "The Exposome and Human Health".

Peng Yin,[‡‡] Cheng He,[‡‡] Renjie Chen,[‡‡] Jianbin Huang, Yong Luo, Xuejie Gao, Ying Xu, John S. Ji, Wenjia Cai, Yongjie Wei, Huichu Li, Maigeng Zhou,* and Haidong Kan*

Cite This: https://doi.org/10.1021/acs.est.3c09162 Read Online

ACCESS | Metrics & More | Article Recommendations | Supporting Information

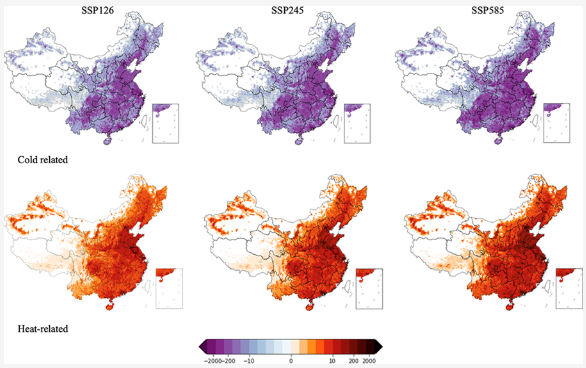

ABSTRACT: The updated climate models provide projections at a fine scale, allowing us to estimate health risks due to future warming after accounting for spatial heterogeneity. Here, we utilized an ensemble of high-resolution (25 km) climate simulations and nationwide mortality data from 306 Chinese cities to estimate death anomalies attributable to future warming. Historical estimation (1986−2014) reveals that about 15.5% [95% empirical confidence interval (eCI):13.1%,17.6%] of deaths are attributable to nonoptimal temperature, of which heat and cold corresponded to attributable fractions of 4.1% (eCI:2.4%, 5.5%) and 11.4% (eCI:10.7%, 12.1%), respectively. Under three climate scenarios (SSP126, SSP245, and SSP585), the national average temperature was projected to increase by 1.45, 2.57, and 4.98 °C by the 2090s, respectively. The corresponding mortality fractions attributable to heat would be 6.5% (eCI:5.2%, 7.7%), 7.9% (eCI:6.3%, 9.4%), and 11.4% (eCI:9.2%, 13.3%). More than half of the attributable deaths due to future warming would occur in north China and cardiovascular mortality would increase more drastically than respiratory mortality. Our study shows that the increased heat-attributable mortality burden would outweigh the decreased cold-attributable burden even under a moderate climate change scenario across China. The results are helpful for national or local policymakers to better address the challenges of future warming.

KEYWORDS: *climate change, nonoptimal temperature, mortality burden*

INTRODUCTION

Over the past few decades, the global average temperature has increased significantly due to climate change.[1] The general rise in land surface temperature, accompanied by the increased heatwave frequency and intensity, leads to a wide range of adverse health outcomes.[2] Our previous study suggested that nonoptimum ambient temperature could account for 14.3% of nonaccidental mortality across China, with cold temperature accounting for 11.6% and heat temperature for 2.7%.[3] Similar estimates on temperature-related mortality burden were reported in the USA,[4] Europe, Australia, and the globe.[5] For future climate change, different geographic characteristics and magnitude of climate warming would lead to an enhanced or weakened long-term net risk.[6] Understanding the changes in temperature-related mortality burden under future climate scenarios and their regional differences are particularly important for developing adequate mitigation and adaptation measures of climate change.[7] Due to the inevitability and variability of future warming, it is urgent to provide an overall assessment of the relative changes in cold- and heat-related mortality, which is useful for guiding the optimal national adaptation strategies and the distribution of medical resources in addressing climate change.

Previous studies have projected changes in mortality burden due to future temperature changes. The majority of these studies focused on the mortality risk associated with ambient heat.[8−10] However, the mortality risks associated with cold or a full range of temperatures were less projected. Previous studies revealed a declining trend for cold-attributable mortality due to future warming in many locations in China[11,12] or regions across the world,[8,13] but these studies were mostly conducted within single locations or regions with limited spatial representativeness. In addition, the existing large-scale

Received: November 3, 2023
Revised: March 10, 2024
Accepted: March 19, 2024

projection studies considered a region or a country as one point for the evaluation,[14,15] ignoring the heterogeneity of temperature changes and vulnerability in different subregions. Given the disproportionately higher disease burden of cold temperatures than hot temperatures, the variations of both cold and hot temperatures under future climate change would significantly affect the projections of the total disease burden. This phenomenon, however, has not been well investigated at a fine scale, which may lead to an inaccurate estimate of the overall disease burden of climate change, especially under the different magnitudes of warming in various regions. Accordingly, the health burden of climate change may be over- or underestimated if the spatial heterogeneity was not appropriately accounted for.

Therefore, the present study was designed to assess the excess deaths attributable to nonoptimum temperatures (both cold and hot temperatures) under multiple climate change scenarios at a grid size of 25 km. We analyzed a nationwide data set of daily mortality and temperature in 306 representative cities at the prefecture level or above in mainland China using a three-stage analytical method.

■ MATERIALS AND METHODS

Data Acquisition. *Daily Mortality and Temperature.* Daily mortality data from 2013 to 2015 was obtained from the China's Disease Surveillance Point System database. We included 306 cities at the prefecture or above with complete daily environmental monitoring data. These cities were selected from the death registry of China's Disease Surveillance Points System. The selection of surveillance points, both at the national and provincial levels, was carried out through a multistage stratification method that carefully considered the sociodemographic characteristics prevalent across the Chinese population, ensuring that the data from these cities could represent different socioeconomic and demographic conditions throughout China.[16] Leveraging data from these cities, we have already studied the varying impacts of temperature and air pollution on the health outcomes of the Chinese population.[3,17] Overall, our data set incorporated both urban and rural deaths and was also nationally representative in China. We extracted deaths due to nonaccidental causes (the International Classification of Diseases-10 (ICD-10) codes A00-R99), cardiovascular diseases (ICD-10: I60−I69), and respiratory diseases (ICD-10: J00-J99) for the 306 cities. Overall, the 306 cities are distributed according to the socioeconomic characteristics of China (Figure S5). Our data set accounts for 92% of all cities at the prefecture or above (total = 334) and covers 95.21% of the total population in mainland China.

The daily mean temperature for each city from 2013 to 2015 was obtained from the ERA5-Land climate reanalysis with 0.1 × 0.1° spatial resolution[18] to estimate the ambient temperature exposure for each location. As ERA5-Land involves data assimilation techniques, it generates very similar temperature distributions to station observations.[19] Many epidemiological studies have validated the use of ERA5-Land data to depict temperature exposure in different locations across the world.[20,21]

Daily Temperature Projection under Different Climate Change Scenarios. For a robust quantification of the daily temperature change, ensembles consisting of more than one single-model initial condition are essential.[22] As shown in Table S1, our study includes data from 10 general circulation models (GCMs) under the historical scenario (1986 to 2014) and future scenarios (2015 to 2100) from the Coupled Model Intercomparison Project Phase 6 (CMIP6). In order to account for a wide range of potential GHG emission changes in the future, we selected three climate change scenarios, i.e., SSP126, SSP245, and SSP585. According to previous studies,[23,24] SSP126 assumes that the changes in radiative forcing are expected to get to 2.6 W/m^2 by 2100, and was designed with the aim of simulating a development that is compatible with the 2 °C targets; SSP245 represents the scenario with an additional radiative forcing of 4.5 W/m^2 by the year 2100, which assumed a medium pathway for future greenhouse gas emissions with certain measures of climate protection; and similarly, SSP585 represents the scenario with an additional radiative forcing of 8.5 W/m^2 by the year 2100, which represents the upper boundary of the range of scenarios described previously[23,25]

The daily temperature series from 10 GCMs were obtained from the latest version of the NASA Earth Exchange Global Daily Downscaled Projections (NEX-GDDP-CMIP6).[26] This downscaled product was generated using a daily variant of the bias correction/spatial disaggregation (BCSD) method and is at 1/4-degree horizontal resolution (approximately 25 km over China).[26] This data set has been widely adopted in projection studies.[27] We selected the daily average temperature series during the historical period (1986−2014) and future period (2015−2100) under three climate change scenarios as we explained above.

As we applied the modeled temperature series to the exposure−response functions established by the temperature series of the ERA5-Land data set, the difference between these two data sets cannot be ignored. So, we additionally corrected modeled temperature series from 10 GCMs based on the temperature series of the ERA5-Land data set using the bias correction method developed by the Inter-Sectoral Impact Model Intercomparison Project.[28] To quantify the accuracy of the temperature series, we employed a Taylor diagram, consisting of the correlation coefficient, root mean square error (RMSE), and the ratio of standard deviation,[29] to facilitate temperatures from the ERA5-Land data set against simulated daily temperature over 306 selected cities. As shown in Figure S6, the RMSEs are mostly within 3 °C, so the modeling output for each GCM during the baseline can well capture the temperature after all of the corrections. They also had the ability to capture temperature variations under different climate change scenarios.

Climate Classification. Based on the Köppen−Geiger climate classification[30] and the existing classification results from a previous study,[31] we first divided all grids into six zones, including Temperate (three subcategories: Cfa, Cwa, and Cwb), Cold (Dwb), Arid (BSk), and Polar (ET). According to the scheme symbols from the Köppen−Geiger climate classification, the first "B", "C", "D", and "E" represent the Arid, Temperate, Cold, and Polar climates, respectively; the second "f", "w", "S", and "T" represent the no dry season, dry winter, steppe, and tundra sub climates, respectively; and the last "a", "b", and "k" represent hot summer, warm summer, and overall cold, respectively. As the total area of the Tropic zone is smaller than 1000 km^2, we reclassified it as the nearest Temperate zone. In addition, climate zones, in which the difference between the highest and lowest mean temperature exceeds 10 °C, were further subcategorized into two subzones based on the median temperature. Overall, all grids were

Table 1. Summary Statistics on Deaths and Annual Mean Temperatures, Classified by Climatic Zones

region	number of cities	total number of deaths	daily mean temperature (±annual standard deviation)
temperate			
no dry season, hot summer			
T_{mean} lower than 50% quantile (Cfa_below)	47	964,336	17.3 (±7.8)
T_{mean} higher than 50% quantile (Cfa_above)	36	562,897	19.5 (±13.4)
dry winter, hot summer			
T_{mean} lower than 50% quantile (Cwa_below)	43	934,612	17.3 (±7.9)
T_{mean} higher than 50% quantile (Cwa_above)	26	361,292	22.2 (±11.3)
dry winter, warm summer (Cwb)	6	71,968	13.8 (±5.3)
cold			
T_{mean} lower than 50% quantile (Dwb_below)	31	361,265	5.8 (±8.1)
T_{mean} higher than 50% quantile (Dwb_above)	57	1,267,473	12.1 (±11.9)
arid			
T_{mean} lower than 50% quantile (BSk_below)	22	131,652	6.6 (±11.0)
T_{mean} higher than 50% quantile (BSk_above)	21	184,295	12.7 (±6.4)
polar (ET)	16	18,119	−0.8 (±4.3)
total	306	4,857,909	

divided into 10 climate categories (Table 1 and Figure S2), including Temperate (three subcategories: Cfa_above, Cfa_below, Cwa_above, Cwa_below, and Cwb), Cold (Dwb_below and Dwb_above), Arid (BSk_below and BSk_above), and Polar (ET). The mean temperature for each grid during the historical period (1986–2014) was extracted and calculated based on the ERA5-Land data set.[18]

Statistical Analysis. *Temperature–Mortality Relationship.* We used a three-stage approach to estimate the association between nonoptimal temperature and daily mortality due to total nonaccidental causes, cardiovascular diseases, and respiratory diseases,[32] ensuring consistency in analysis method and model parameter settings for all of these three outcomes. Specifically, in the first stage, we used the overdispersed generalized linear model with quasi-Poisson regression and distributed lag nonlinear model (DLNM) to obtain the exposure–response relationship between daily mean temperature and mortality for each of the 306 Chinese cities. Following the DLNM framework in our previous studies,[33,34] we built a cross-basis function using quadratic B splines with three knots at the 10th, 75th, and 90th percentiles of daily temperature and natural cubic splines with an intercept and three equally spaced knots for lags up to 21 days to capture possible lagged and nonlinear relationships. As for covariates, we controlled for calendar days in natural cubic splines with 12 degrees of freedom per year to control for seasonality and long-term trends, same-day relative humidity in natural cubic spline with 3 degrees of freedom, and a categorical variable of the day of the week.

In the second stage, we fitted a multivariate meta-regression model for the reduced cumulative association for each location with geospatial predictors that have been previously shown to explain the majority of the heterogeneity in the relationships between ambient temperature and mortality.[3,35] These predictors included climate zones classified based on the Köppen–Geiger approach,[36] annual mean temperature, and standard deviation of daily mean temperature.

In the third stage, we predicted the associations of daily temperature and mortality for each 25 km grid using the meta-regression model and the above predictors measured at each grid. We used the minimum mortality temperature (MMT) as a reference for each predicted temperature–mortality relationship.

The population size of each grid was calculated by averaging the population counts at a 1 km resolution that were extracted from the WorldPop data set.[37] We included only grids with more than one death per year. Finally, a total of 11,420 grids were included, covering 99.996% of China's total population.

Projection of Temperature-Related Mortality. Temperature-related mortality in each grid was calculated using the formula below.[38,39] Specifically, for grid i on day d, the attributable deaths due to nonoptimal temperature on day d (TD_{id}) were calculated as

$$TD_{id} = \frac{(RR_{id} - 1)}{RR_{id}} \times POP \times D_i$$

where RR_{id} is the cumulative relative risk extracted from the grid-specific temperature–mortality association, which was predicted in the third stage and by the simulated daily temperature in grid i on day d. POP is the average annual population in grid i. D_i represents the daily death rate at the provincial level. Due to the unavailability of baseline daily mortality data for all cities within China, we resorted to using provincial-level data as a proxy.

We then calculated the attributable fraction in each grid using the ensembled daily temperature projection for the historical and various future scenarios.[38] The 95% empirical confidence intervals (eCIs) were calculated by Monte Carlo simulations (500 samples) to quantify the uncertainty in the estimation of the exposure–response relationships and the variability in temperature projections between three GCMs.

In addition, we further divided all days during historical and future periods into extreme cold [Daily mean temperature (T_{mean}) ≤ 2.5th percentile in the baseline period], moderate cold (2.5th percentile in the observational period < T_{mean} ≤ MMT), moderate heat (MMT < T_{mean} < 97.5 percentile in the baseline period), and extreme heat (97.5th percentile in the baseline period ≤ T_{mean}). These thresholds will be used to subcategorize the mortality burden for nonoptimal temperature under these scenarios.

■ RESULTS

Descriptive Data. We included a total of 4,857,909, 2,445,673, and 712,480 deaths from nonaccidental causes, cardiovascular diseases, and respiratory diseases from 306 cities in mainland China during the baseline period (2013–2015).

https://doi.org/10.1021/acs.est.3c09162
Environ. Sci. Technol. XXXX, XXX, XXX−XXX

Table 1 shows the summary statistics about the number of deaths, annual average daily mean temperature, and their standard deviations over 10 climate categories. The mean temperature during the baseline ranged from −0.8 °C in the ET to 22.2 °C in the Cwa_above.

Region-Specific Temperature–Mortality Relationships. The national exposure–response curves (Figure S1) were generally inversely J-shaped for the associations of daily mean temperature with total nonaccidental, cardiovascular, and respiratory mortality. Under extreme heat conditions (i.e., 95th of the daily mean temperature), the relative risk (RR) of cardiovascular mortality is higher than that of total mortality and respiratory mortality.

Figure 1 depicts the minimum mortality temperature (MMT) at daily mean levels for 10 climate zones. The distribution of MMT varied considerably by region from 16 to 30 °C. We observed higher MMTs in warm regions such as Cwa and Cfa, and lower MMTs in cool regions such as ET. In addition, there was a significant and positive relationship between annual mean temperature and MMTs across different areas ($r = 0.83$), which is consistent with a recent study.[40] Table S2 presents the results of meta-regression analyses in the associations of mortality associated with nonoptimum temperature.

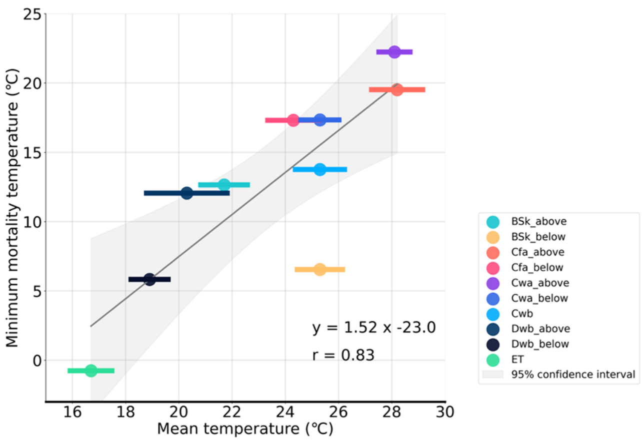

Figure 1. Pooled minimum mortality temperatures by climatic zones in China. The order of the y-axis is sorted according to the average temperature for each climate zone. Cwa represents the Temperate climate zone with dry winter and hot summer; Cfa represents the Temperate climate zone with no dry season and hot summer; Cwb represents the Temperate climate zone with dry winter and warm summer; Dwb represents the Cold climate zone; BSk represents the Arid climate zone; ET represents the Polar climate zone. "_above" represents the annual temperature higher than 50% quantile of all temperatures across all climate zone, "_below" represents the annual temperature lower than 50% quantile of all temperatures across all climate zones. There is a significant and positive correlation between minimum mortality temperatures and annual mean temperature with $r = 0.83$ and slope = 1.52 in the simple linear regression model.

Temporal and Spatial Trends in Future Temperatures. Figures 2 and S2 depict the temporal and spatial distribution of the mean annual temperature anomalies by three SSPs over four main climate zones. Overall, mean temperatures will increase drastically, modestly, and slightly in the SSP585, SSP126, and SSP245 scenarios after the middle of this century, respectively. By the end of this century (the 2090s), the average temperature would rise by 1.45 °C under SSP126, 2.57 °C under SSP245, and 4.98 °C under SSP585, compared to the historical period (1986–2014). As shown in Table S3, cooler regions, such as the Cold and Arid zones, tend to experience more prominent warming, whereas the warmest region (Temperate) tends to have modest warming in the 2090s.

Future Mortality Burden. Under future warming scenarios, the cold-related attributable fraction is expected to drop, and the heat-related attributable fraction will experience a drastic increase (Figures S3 and S4). As shown in Figure 3, the total attributable fraction due to both cold and heat temperatures will experience a plateau after the 2050s in SSP126 and SSP245, and consistently increase throughout the 21st century under SSP585. In addition, by the end of this century, the total attributable fraction for cardiovascular deaths will increase more than that for respiratory deaths. For nonaccidental, cardiovascular, and respiratory deaths, the increases in the heat-related attributable fraction are projected to offset the decline in cold-related attributable fraction, making the total attributable net deaths increase even under the SSP246 scenario.

Tables S4–S6 summarize the projected decreases in cold-related deaths and increases in heat-related deaths due to future warming by the 2090s compared to the historical period under the SSP126, SSP245, and SSP585 scenarios. Across all climate zones, we projected a reduction of 33,400 overall deaths under SSP126, whereas an increment of 9,703 and 17,503 overall temperature-related deaths under SSP245 and SSP585, respectively. Over the four regions, the Temperate zone was projected to witness the largest decrease in cold-attributable deaths and the largest increase in heat-attributable deaths under SSP585. Under SSP245 and SSP126, the Cold zone had the largest number of heat-attributable deaths.

Figure 4 shows the projection of cold and heat-attributable deaths by various SSP scenarios during the 2090s compared with the baseline period. By regions, this spatial distribution is largely coincident with the spatial pattern of vulnerability (Figure 1) and modeled average warming (Figure S2) among regions. The spatial distribution is similar among the three scenarios, but the magnitudes are largely different (Figure 5).

We further subcategorized the attributable mortality fractions into moderate and extreme cold or hot temperatures. Over the historical period, the moderate cold could account for the largest mortality fraction and extreme heat could account for the smallest fraction. Under the three climate scenarios, the mortality fraction attributable to moderate cold was projected to decrease most drastically, while the attributable fraction of extreme heat would increase most significantly under SSP585. In addition, the attributable fraction of extreme cold and moderate heat would remain constant under SSP126. Moreover, by the end of this century, the attributable fraction of extreme heat is projected to be higher than that of moderate cold under SSP585.

DISCUSSION

We estimated the nationwide mortality risk and burden due to future climate change at a grid size of 25 km and depicted its temporal patterns under three different climate change scenarios. Totally, about 250,992 nonaccidental deaths are attributable to nonoptimal temperature per year during the historical period (1986–2014), with the cold being more harmful than heat and cardiovascular diseases more sensitive to heat than respiratory diseases. In terms of future change, our

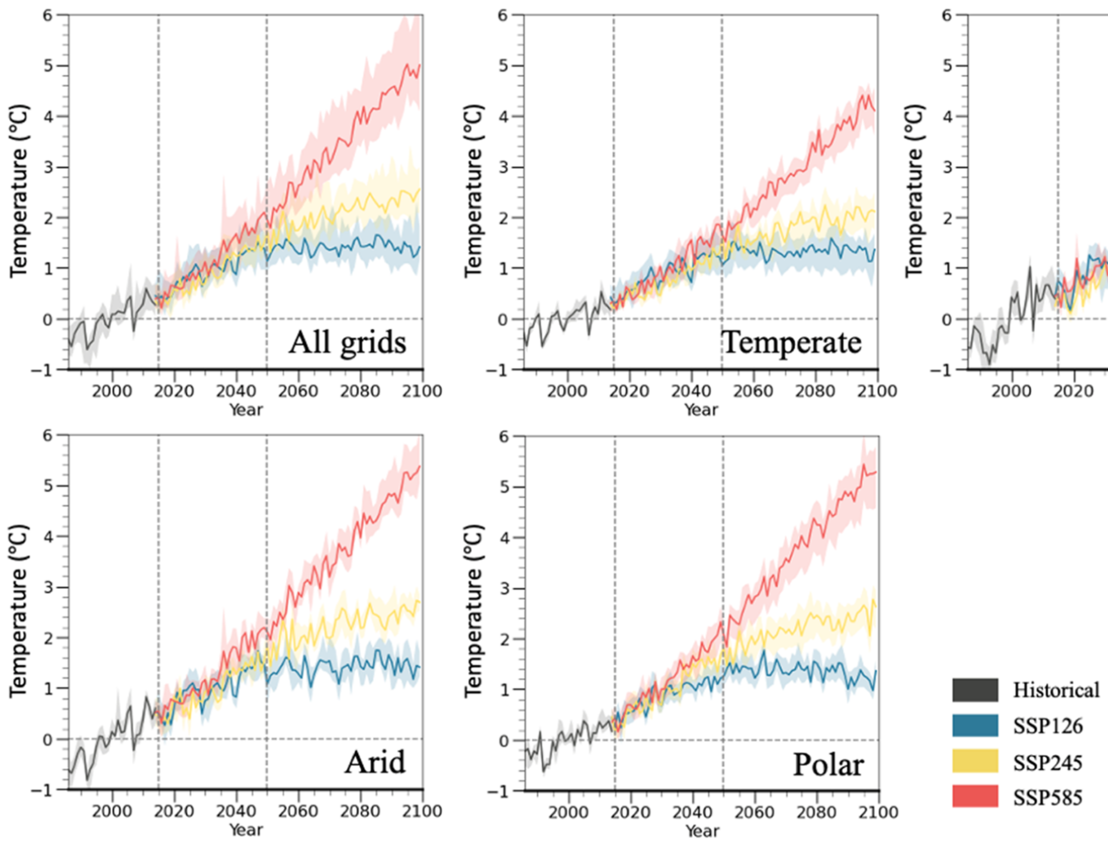

Figure 2. Projected changes in annual mean temperature compared to the reference period (1986–2014) by various climate change scenarios across four climate zones and all grids. The colored area represents the interquartile range of changes across the regions.

study projected a reduction in the cold-attributable mortality fraction and a significant increase in the heat-attributable fraction. In addition, the overall heat-attributable mortality fraction for cardiovascular diseases was expected to increase at a magnitude higher than that for respiratory diseases. Overall, the heat-related burden increase was expected to outweigh the cold-related burden decrease under the medium-emission scenario (SSP245) and high-emission scenario (SSP585) across China, especially for mortality due to cardiovascular diseases. Our results revealed that the overall mortality burden would remain stable only under the low-emission scenario for all regions, highlighting the crucial role of controlling greenhouse gas emissions.

Our results are comparable to previous studies conducted in developed countries.[6,7,41] One study involving 16 European countries reported the increments in the heat-attributable mortality fraction would exceed the decrements in the cold-attributable fraction under RCP8.5.[39] The baseline mortality burden attributed to nonoptimum ambient temperature calculated in this study is consistent with our previous study[3] and the total number of attributable deaths is close to a regional estimate of excess deaths over East Asia from a global scale study.[35] For the projected changes in heat-related mortality under different climate scenarios, our results were also largely similar to previous studies.[14,42] In addition, a recent study across 105 counties in China and other projection studies in different areas across China also projected similar cold- and heat-related mortality burdens.[11,12,43] However, some of these projection studies did not account for the overall changes in temperature-related mortality burden, and some of them were also unable to compare the changes over different regions under various scenarios. More importantly, most of the previous projection studies failed to appropriately account for the spatial heterogeneity over such a large population. Considering the immense and dynamically changing population base in China, coupled with the country's complex climatic conditions that vary from coastal to inland regions and from monsoon to continental climates, the impacts of future climate changes are expected to be significantly different across regions. These variations will likely be influenced by diverse geographic latitudes, humidity conditions, and altitudinal differences. Consequently, previous research, often based on data from a limited selection of urban residents or certain representative locations, has not been able to portray the extensive and profound impacts of climate change. To our knowledge, this analysis is the first study that accounted for the overall changes in temperature-related mortality burden across China, a nation with a large and rapidly transitioning population, at a fine spatial scale of less than 100 km. Furthermore, we have compared the future trends of major mortality outcomes across varying emission scenarios, providing a scientific foundation for devising more precise response strategies and future planning for different regions across China.

By regions, we found that local minimum mortality temperatures were associated with the regional annual mean temperatures. Accordingly, the regional differences in local resident vulnerability could affect the current estimation of the temperature-related mortality burden and strongly determine their projections under future climate change scenarios across various locations in China. In terms of future changes, our projection analysis with high spatial resolution revealed that

https://doi.org/10.1021/acs.est.3c09162
Environ. Sci. Technol. XXXX, XXX, XXX−XXX

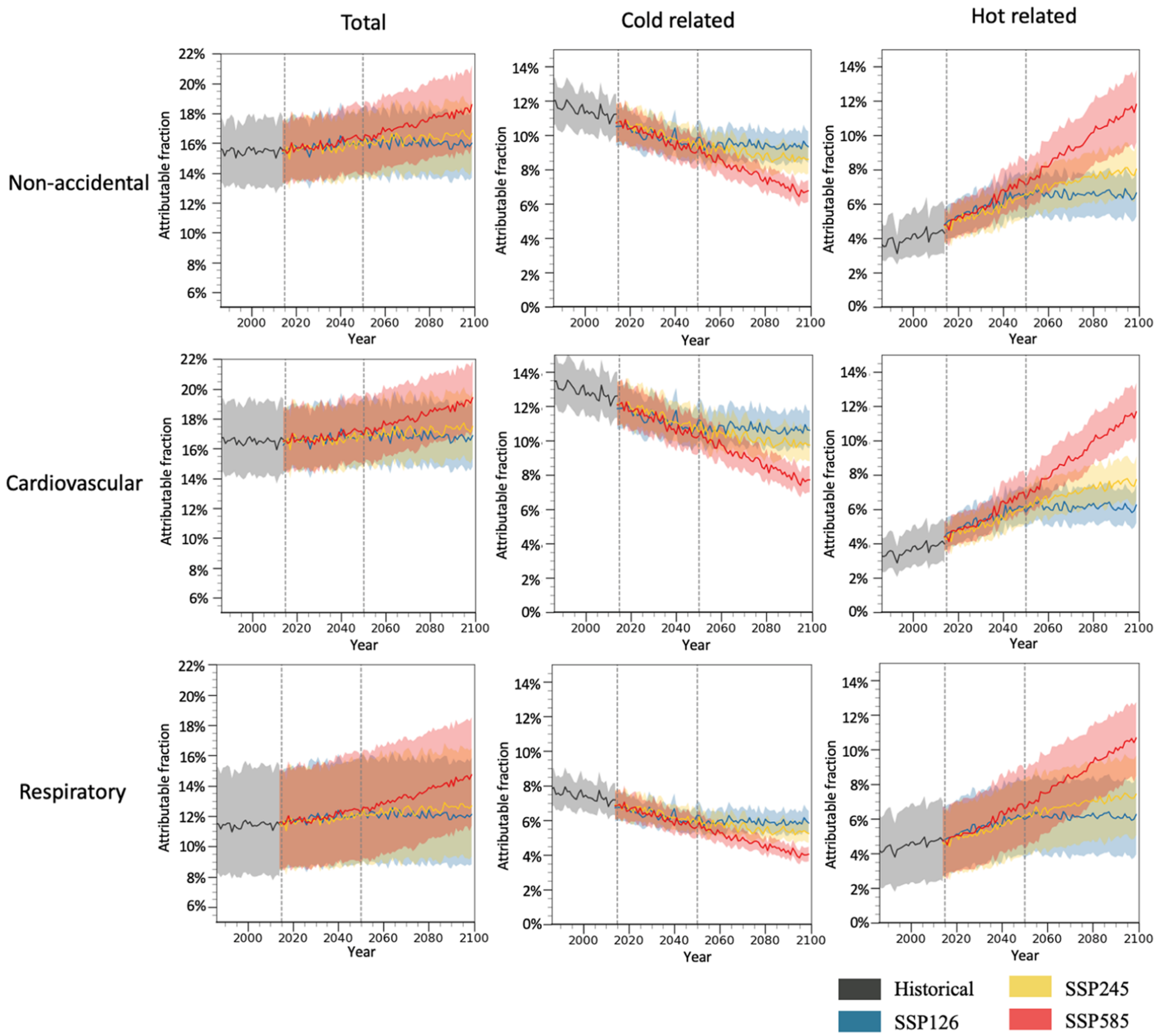

Figure 3. Projections of attributable fractions of mortality due to nonoptimum temperature (including total, cold-related, and hot-related) from total nonaccidental causes, cardiovascular diseases, and respiratory diseases, by climate change scenarios across China and four climate regions. Projections were derived from the averages of the 10 general circulation models (GCMs). The shaded areas are the 95% empirical confidence intervals.

cold-related deaths would decrease most markedly in south China (the Temperate zone), while heat-related deaths would increase most significantly in north China (including the Cold and Arid zones). In the Polar zone, we projected a substantial decrease in cold-related mortality fractions due to its severe warming. Nationally, future heat and cold temperatures would notably change the composition of the overall mortality burden attributable to nonoptimum temperature. We projected that more than half of the excess deaths attributable to future temperature changes would occur in north China, which means that the net burden due to future heat exposure would overshadow the reduction of the cold-related burden in this region. This result underlined the disproportionately high disease burden attributable to climate change in northern cities. In contrast, south China will experience the smallest increment of the temperature-related mortality burden. It is noteworthy that we projected a large quantity of heat-attributable deaths occurring in populous cities along the southeast coastline. The geographical heterogeneity of future disease burden suggests that tailored adaptation strategies for each region are important to better address the public health challenges of climate change.

The present study has several notable strengths and significance. First, we estimated the exposure−response relationship between daily temperatures and all-cause or cause-specific mortality using a well-representative, large-scale data set. Second, our nationwide data set was characterized by various demographical, climatic, and socioeconomic conditions, offering an opportunity to explore the spatial heterogeneity of the susceptibility to climate change. Third, different from most previous studies confined to the region-level estimations,[14,15] this study projected mortality burden at a fine spatial resolution of 25 km × 25 km and provided ample evidence on the differential disease burden due to future

https://doi.org/10.1021/acs.est.3c09162
Environ. Sci. Technol. XXXX, XXX, XXX−XXX

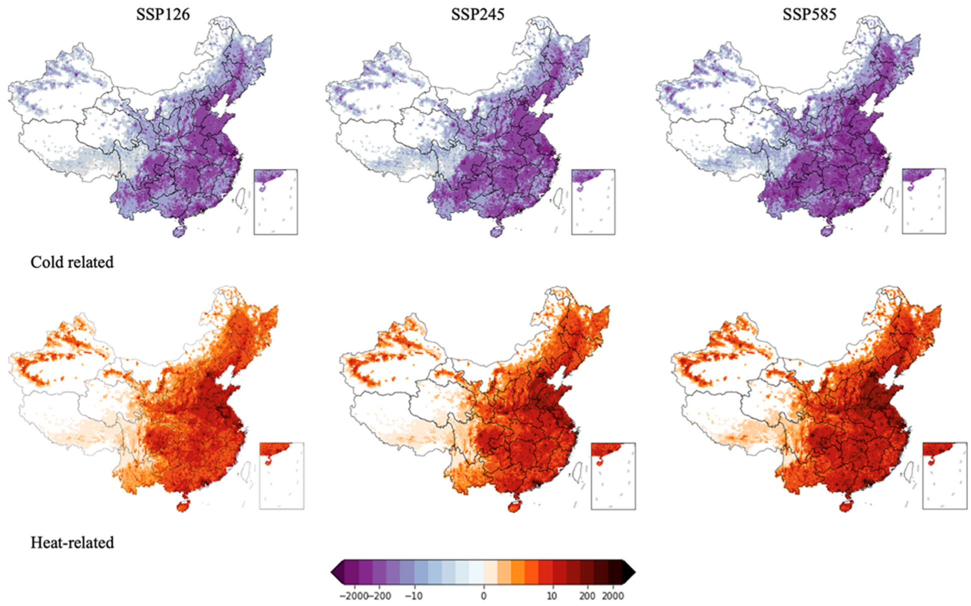

Figure 4. Projections of changes in annual attributable deaths due to cold and heat temperatures in the 2090s compared to the reference period (1986–2014), classified by climate change scenarios at a grid scale with 25 km spatial resolution.

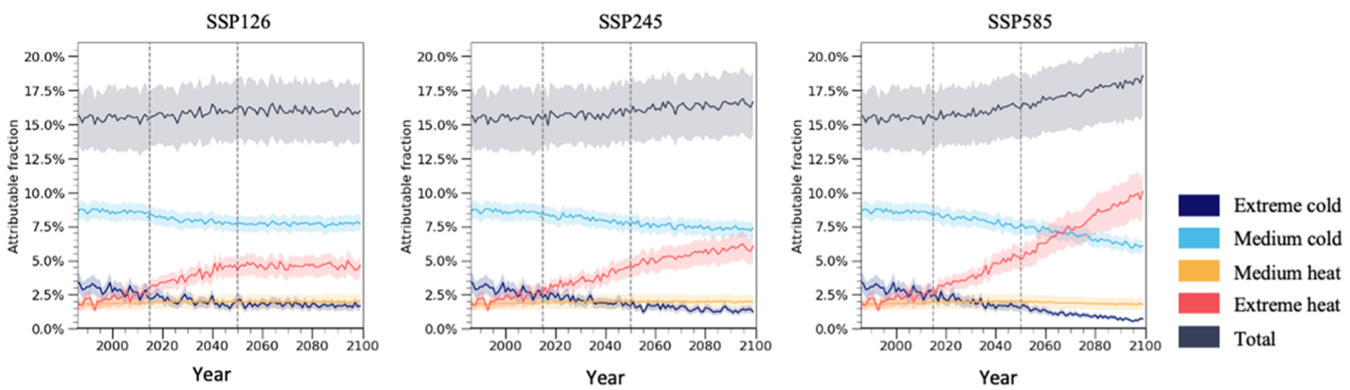

Figure 5. Projections of mortality fractions attributable to nonoptimum temperatures compared to the reference period (1986–2014), by climate change scenarios across China. Projections were presented as the averages of 10 general circulation models (GCMs). The shaded areas are 95% empirical confidence intervals.

warming in various subregions. These results are helpful for national or local policymakers to develop tailored adaptation plans and efficient health protection strategies to better address the challenges of future warming. Finally, our assessment formed a more comprehensive understanding of how future climate change affects both heat- and cold-related mortality burdens across China or regions with similar climate conditions.

Nevertheless, our study still has some limitations. First, we did not consider other potential effect modifiers (such as economic conditions, age, and sex structure) in estimations of temperature–mortality associations across locations due to the lack of data at the fine scale. In addition, although our results could be reasonably extrapolated to the entire China, we could not separate our aggregate death data into urban and rural areas, limiting our ability to explore the possible differences of disease burden projections between urban and rural areas. Second, the assumption of no changes in population distributions allows us to estimate the mortality risk purely caused by future climate change. However, it may lead to some overestimation or underestimation of the projected disease burden probably due to any unexpected changes in the urbanization process and total population size.[44] Third, our time-series death database covered only 3 years (from 2013 to 2015), which is somewhat short and may attenuate the stability of baseline risk estimations. Lastly, consistent with most previous studies,[6,39] we projected attributable disease burden under the assumption of no adaptation, and thus this assumption could add uncertainty to our results because the knowledge of future vulnerability or adaptation ability is largely unknown,[45] and the MMT can also change over time.[46]

In summary, this nationwide study revealed that the increased heat-attributable mortality burden would outweigh the decreased cold-attributable burden, even under a moderate climate change scenario across China. This kind of imbalance would also vary by geographical and climatic zones. Our findings demonstrated that an assessment of overall disease burden attributable to future temperature change at a fine spatial resolution is crucial to accurately estimate the health cost of climate warming and evaluate national or regional climate policies, such as carbon peaking and a carbon neutrality plan.

https://doi.org/10.1021/acs.est.3c09162
Environ. Sci. Technol. XXXX, XXX, XXX−XXX

■ ASSOCIATED CONTENT

Data Availability Statement

Data were collected within the Disease Surveillance Point System database under a data-sharing agreement and cannot be made publicly available.

Supporting Information

The Supporting Information is available free of charge at https://pubs.acs.org/doi/10.1021/acs.est.3c09162.

Key information on the climate models used; background climatic conditions of the study area; and changes in the burden of various major health outcomes in the future (PDF)

■ AUTHOR INFORMATION

Corresponding Authors

Maigeng Zhou − *National Center for Chronic and Noncommunicable Disease Control and Prevention, Chinese Center for Disease Control and Prevention, Beijing 100050, China*; Email: maigengzhou@126.com

Haidong Kan − *School of Public Health, Shanghai Institute of Infectious Disease and Biosecurity, Key Lab of Public Health Safety of the Ministry of Education and NHC Key Lab of Health Technology Assessment, Fudan University, Shanghai 200082, China; National Center for Children's Health, Children's Hospital of Fudan University, Shanghai 200032, China*; orcid.org/0000-0002-1871-8999; Email: kanh@fudan.edu.cn

Authors

Peng Yin − *National Center for Chronic and Noncommunicable Disease Control and Prevention, Chinese Center for Disease Control and Prevention, Beijing 100050, China*; orcid.org/0000-0002-5515-2824

Cheng He − *School of Public Health, Shanghai Institute of Infectious Disease and Biosecurity, Key Lab of Public Health Safety of the Ministry of Education and NHC Key Lab of Health Technology Assessment, Fudan University, Shanghai 200082, China; Institute of Epidemiology, Helmholtz Zentrum München—German Research Center for Environmental Health (GmbH), Neuherberg 85764, Germany*; orcid.org/0000-0002-8470-0834

Renjie Chen − *School of Public Health, Shanghai Institute of Infectious Disease and Biosecurity, Key Lab of Public Health Safety of the Ministry of Education and NHC Key Lab of Health Technology Assessment, Fudan University, Shanghai 200082, China*

Jianbin Huang − *Department of Earth System Science, Ministry of Education Key Laboratory for Earth System Modeling, Institute for Global Change Studies, Tsinghua University, Beijing 100084, China*

Yong Luo − *Department of Earth System Science, Ministry of Education Key Laboratory for Earth System Modeling, Institute for Global Change Studies, Tsinghua University, Beijing 100084, China*

Xuejie Gao − *College of Earth and Planetary Sciences, University of Chinese Academy of Sciences, Beijing 100049, China; Climate Change Research Center, Institute of Atmospheric Physics, Chinese Academy of Sciences, Beijing 100017, China*

Ying Xu − *National Climate Center, China Meteorological Administration, Beijing 100044, China*

John S. Ji − *Vanke School of Public Health, Tsinghua University, Beijing 100084, China*; orcid.org/0000-0002-5002-118X

Wenjia Cai − *Department of Earth System Science, Ministry of Education Key Laboratory for Earth System Modeling, Institute for Global Change Studies, Tsinghua University, Beijing 100084, China*; orcid.org/0000-0002-4436-512X

Yongjie Wei − *State Key Laboratory of Environmental Criteria and Risk Assessment, Chinese Research Academy of Environmental Sciences, Beijing 100012, China*

Huichu Li − *Department of Environmental Health, Harvard T.H. Chan School of Public Health, Boston, Massachusetts 02115, United States*

Complete contact information is available at: https://pubs.acs.org/10.1021/acs.est.3c09162

Author Contributions

[‡‡]P.Y., C.H., and R.C. contributed equally to this work.

Funding

This study was supported by the National Natural Science Foundation of China (82030103), the National Key Research and Development Program of China (2022YFC3702701), the Shanghai International Science and Technology Partnership Project (21230780200), and the Shanghai Committee of Science and Technology (21TQ015). C.H. gratefully acknowledges support from the Alexander von Humboldt Foundation for the Humboldt Research Fellowship.

Notes

The authors declare no competing financial interest.

■ REFERENCES

(1) Pörtner, H.-O.; Roberts, D. C.; Adams, H.; Adler, C.; Aldunce, P.; Ali, E.; Begum, R. A.; Betts, R.; Kerr, R. B.; Biesbroek, R. *Climate Change 2022: Impacts, Adaptation and Vulnerability*; IPCC, 2022.

(2) Gasparrini, A.; Guo, Y.; Hashizume, M.; Lavigne, E.; Zanobetti, A.; Schwartz, J.; Tobias, A.; Tong, S.; Rocklöv, J.; Forsberg, B.; et al. Mortality risk attributable to high and low ambient temperature: a multicountry observational study. *Lancet* **2015**, *386* (9991), 369−375, DOI: 10.1016/S0140-6736(14)62114-0.

(3) Chen, R.; Yin, P.; Wang, L.; Liu, C.; Niu, Y.; Wang, W.; Jiang, Y.; Liu, Y.; Liu, J.; Qi, J.; et al. Association between ambient temperature and mortality risk and burden: time series study in 272 main Chinese cities. *BMJ* **2018**, *363*, No. k4306, DOI: 10.1136/bmj.k4306.

(4) Nordio, F.; Zanobetti, A.; Colicino, E.; Kloog, I.; Schwartz, J. J. E. i. Changing patterns of the temperature−mortality association by time and location in the US, and implications for climate change. *Environ. Int.* **2015**, *81*, 80−86.

(5) Murray, C. J. L.; Aravkin, A. Y.; Zheng, P.; Abbafati, C.; Abbas, K. M.; Abbasi-Kangevari, M.; Abd-Allah, F.; Abdelalim, A.; Abdollahi, M.; Abdollahpour, I.; et al. Global burden of 87 risk factors in 204 countries and territories, 1990−2019: a systematic analysis for the Global Burden of Disease Study 2019. *Lancet* **2020**, *396* (10258), 1223−1249.

(6) Gasparrini, A.; Guo, Y.; Sera, F.; Vicedo-Cabrera, A. M.; Huber, V.; Tong, S.; de Sousa Zanotti Stagliorio Coelho, M.; Saldiva, P. H. N.; Lavigne, E.; Correa, P. M.; et al. Projections of temperature-related excess mortality under climate change scenarios. *Lancet Planet. Health* **2017**, *1* (9), e360−e367, DOI: 10.1016/S2542-5196(17)30156-0.

(7) Vicedo-Cabrera, A. M.; Guo, Y.; Sera, F.; Huber, V.; Schleussner, C.-F.; Mitchell, D.; Tong, S.; de Sousa Zanotti Staglior Coelho, M.; Saldiva, P. H. N.; Lavigne, E.; et al. Temperature-related mortality impacts under and beyond Paris Agreement climate change scenarios.

Clim. Change **2018**, *150* (3), 391−402, DOI: 10.1007/s10584-018-2274-3.

(8) Vicedo-Cabrera, A. M.; Sera, F.; Guo, Y.; Chung, Y.; Arbuthnott, K.; Tong, S.; Tobias, A.; Lavigne, E.; de Sousa Zanotti Stagliorio Coelho, M.; Saldiva, P. H. N.; et al. A multi-country analysis on potential adaptive mechanisms to cold and heat in a changing climate. *Environ. Int.* **2018**, *111*, 239−246, DOI: 10.1016/j.envint.2017.11.006.

(9) Achebak, H.; Devolder, D.; Ballester, J. Heat-related mortality trends under recent climate warming in Spain: A 36-year observational study. *PLoS Med.* **2018**, *15* (7), No. e1002617, DOI: 10.1371/journal.pmed.1002617.

(10) Achebak, H.; Devolder, D.; Ballester, J. Trends in temperature-related age-specific and sex-specific mortality from cardiovascular diseases in Spain: a national time-series analysis. *Lancet Planet. Health* **2019**, *3* (7), e297−e306, DOI: 10.1016/S2542-5196(19)30090-7.

(11) Zhu, D.; Zhou, Q.; Liu, M.; Bi, J. Non-optimum temperature-related mortality burden in China: Addressing the dual influences of climate change and urban heat islands. *Sci. Total Environ.* **2021**, *782*, No. 146760.

(12) Gu, S.; Zhang, L.; Sun, S.; Wang, X.; Lu, B.; Han, H.; Yang, J.; Wang, A. Projections of temperature-related cause-specific mortality under climate change scenarios in a coastal city of China. *Environ. Int.* **2020**, *143*, No. 105889.

(13) Ballester, J.; Robine, J.-M.; Herrmann, F. R.; Rodó, X. Long-term projections and acclimatization scenarios of temperature-related mortality in Europe. *Nat. Commun.* **2011**, *2* (1), No. 358, DOI: 10.1038/ncomms1360.

(14) Yang, J.; Zhou, M.; Ren, Z.; Li, M.; Wang, B.; Liu, D. L.; Ou, C.-Q.; Yin, P.; Sun, J.; Tong, S.; et al. Projecting heat-related excess mortality under climate change scenarios in China. *Nat. Commun.* **2021**, *12* (1), No. 1036, DOI: 10.1038/s41467-021-21305-1.

(15) Wang, Y.; Wang, A.; Zhai, J.; Tao, H.; Jiang, T.; Su, B.; Yang, J.; Wang, G.; Liu, Q.; Gao, C.; et al. Tens of thousands additional deaths annually in cities of China between 1.5 °C and 2.0 °C warming. *Nat. Commun.* **2019**, *10* (1), No. 3376, DOI: 10.1038/s41467-019-11283-w.

(16) Liu, S.; Wu, X.; Lopez, A. D.; Wang, L.; Cai, Y.; Page, A.; Yin, P.; Liu, Y.; Li, Y.; Liu, J.; et al. An integrated national mortality surveillance system for death registration and mortality surveillance, China. *Bull. W.H.O.* **2016**, *94* (1), No. 46, DOI: 10.2471/BLT.15.153148.

(17) Chen, R.; Yin, P.; Meng, X.; Wang, L.; Liu, C.; Niu, Y.; Liu, Y.; Liu, J.; Qi, J.; You, J.; et al. Associations between coarse particulate matter air pollution and cause-specific mortality: a nationwide analysis in 272 Chinese cities. *Environ. Health Perspect.* **2019**, *127* (01), No. 017008.

(18) Muñoz-Sabater, J.; Dutra, E.; Agustí-Panareda, A.; Albergel, C.; Arduini, G.; Balsamo, G.; Boussetta, S.; Choulga, M.; Harrigan, S.; Hersbach, H.; et al. ERA5-Land: A state-of-the-art global reanalysis dataset for land applications. *Earth Syst. Sci. Data* **2021**, *13* (9), 4349−4383.

(19) Mistry, M. N.; Schneider, R.; Masselot, P.; Royé, D.; Armstrong, B.; Kyselý, J.; Orru, H.; Sera, F.; Tong, S.; Lavigne, É.; et al. Comparison of weather station and climate reanalysis data for modelling temperature-related mortality. *Sci. Rep.* **2022**, *12*, No. 5178, DOI: 10.1038/s41598-022-09049-4.

(20) Royé, D.; Íñiguez, C.; Tobías, A. Comparison of temperature−mortality associations using observed weather station and reanalysis data in 52 Spanish cities. *Environ. Res.* **2020**, *183*, No. 109237.

(21) Urban, A.; Di Napoli, C.; Cloke, H. L.; Kyselý, J.; Pappenberger, F.; Sera, F.; Schneider, R.; Vicedo-Cabrera, A. M.; Acquaotta, F.; Ragettli, M. S.; et al. Evaluation of the ERA5 reanalysis-based Universal Thermal Climate Index on mortality data in Europe. *Environ. Res.* **2021**, *198*, No. 111227.

(22) Vicedo-Cabrera, A. M.; Scovronick, N.; Sera, F.; Royé, D.; Schneider, R.; Tobias, A.; Astrom, C.; Guo, Y.; Honda, Y.; Hondula, D. M.; et al. The burden of heat-related mortality attributable to recent human-induced climate change. *Nat. Clim. Change* **2021**, *11* (6), 492−500, DOI: 10.1038/s41558-021-01058-x.

(23) O'Neill, B. C.; Tebaldi, C.; Van Vuuren, D. P.; Eyring, V.; Friedlingstein, P.; Hurtt, G.; Knutti, R.; Kriegler, E.; Lamarque, J.-F.; Lowe, J.; et al. The scenario model intercomparison project (ScenarioMIP) for CMIP6. *Geosci. Model Dev.* **2016**, *9* (9), 3461−3482.

(24) You, Q.; Cai, Z.; Wu, F.; Jiang, Z.; Pepin, N.; Shen, S. S. Temperature dataset of CMIP6 models over China: evaluation, trend and uncertainty. *Clim. Dyn.* **2021**, *57* (1), 17−35.

(25) Kriegler, E.; Edmonds, J.; Hallegatte, S.; Ebi, K. L.; Kram, T.; Riahi, K.; Winkler, H.; Van Vuuren, D. P. A new scenario framework for climate change research: the concept of shared climate policy assumptions. *Clim. Change* **2014**, *122* (3), 401−414.

(26) Thrasher, B.; Wang, W.; Michaelis, A.; Melton, F.; Lee, T.; Nemani, R. NASA Global Daily Downscaled Projections, CMIP6. *Sci. Data* **2022**, *9* (1), No. 262, DOI: 10.1038/s41597-022-01393-4.

(27) Tewari, K.; Mishra, S. K.; Salunke, P.; Dewan, A. Future projections of temperature and precipitation for Antarctica. *Environ. Res. Lett.* **2022**, *17* (1), No. 014029.

(28) Hempel, S.; Frieler, K.; Warszawski, L.; Schewe, J.; Piontek, F. A trend-preserving bias correction−the ISI-MIP approach. *Earth Syst. Dyn.* **2013**, *4* (2), 219−236, DOI: 10.5194/esd-4-219-2013.

(29) Taylor, K. E. Summarizing multiple aspects of model performance in a single diagram. *J. Geophys. Res.: Atmos.* **2001**, *106* (D7), 7183−7192, DOI: 10.1029/2000JD900719.

(30) Peel, M. C.; Finlayson, B. L.; McMahon, T. A. Updated world map of the Köppen-Geiger climate classification. *Hydrol. Earth Syst. Sci.* **2007**, *11* (5), 1633−1644.

(31) Beck, H. E.; Zimmermann, N. E.; McVicar, T. R.; Vergopolan, N.; Berg, A.; Wood, E. F. Present and future Köppen-Geiger climate classification maps at 1-km resolution. *Sci. Data* **2018**, *5* (1), No. 180214, DOI: 10.1038/sdata.2018.214.

(32) Zhao, Q.; Guo, Y.; Ye, T.; Gasparrini, A.; Tong, S.; Overcenco, A.; Urban, A.; Schneider, A.; Entezari, A.; Vicedo-Cabrera, A. M.; et al. Global, regional, and national burden of mortality associated with non-optimal ambient temperatures from 2000 to 2019: a three-stage modelling study. *Lancet Planet. Health* **2021**, *5* (7), e415−e425, DOI: 10.1016/S2542-5196(21)00081-4.

(33) Gasparrini, A. Distributed lag linear and non-linear models in R: the package dlnm. *J. Stat. Software* **2011**, *43* (8), 1−20, DOI: 10.18637/jss.v043.i08.

(34) Chen, R.; Yin, P.; Wang, L.; Liu, C.; Niu, Y.; Wang, W.; Jiang, Y.; Liu, Y.; Liu, J.; Qi, J.; et al. Association between ambient temperature and mortality risk and burden: time series study in 272 main Chinese cities. *BMJ* **2018**, *363*, No. k4306, DOI: 10.1136/bmj.k4306.

(35) Zhao, Q.; Guo, Y.; Ye, T.; Gasparrini, A.; Tong, S.; Overcenco, A.; Urban, A.; Schneider, A.; Entezari, A.; Vicedo-Cabrera, A. M.; et al. Global, regional, and national burden of mortality associated with non-optimal ambient temperatures from 2000 to 2019: a three-stage modelling study. *Lancet Planet. Health* **2021**, *5* (7), e415−e425.

(36) Beck, H. E.; Zimmermann, N. E.; McVicar, T. R.; Vergopolan, N.; Berg, A.; Wood, E. Present and future Köppen-Geiger climate classification maps at 1-km resolution. *Sci. Data* **2018**, *5* (1), No. 180214, DOI: 10.1038/sdata.2018.214.

(37) Tatem, A. J. WorldPop, open data for spatial demography. *Sci. Data* **2017**, *4* (1), No. 170004, DOI: 10.1038/sdata.2017.4.

(38) Vicedo-Cabrera, A. M.; Sera, F.; Gasparrini, A. J. E. Hands-on tutorial on a modeling framework for projections of climate change impacts on health. *Epidemiology* **2019**, *30* (3), 321−329, DOI: 10.1097/EDE.0000000000000982.

(39) Martínez-Solanas, È.; Quijal-Zamorano, M.; Achebak, H.; Petrova, D.; Robine, J.-M.; Herrmann, F. R.; Rodó, X.; Ballester, J. Projections of temperature-attributable mortality in Europe: a time series analysis of 147 contiguous regions in 16 countries. *Lancet Planet. Health* **2021**, *5* (7), e446−e454.

(40) Tobías, A.; Hashizume, M.; Honda, Y.; Sera, F.; Ng, C. F. S.; Kim, Y.; Roye, D.; Chung, Y.; Dang, T. N.; Kim, H. Geographical

variations of the minimum mortality temperature at a global scale: a multicountry study. *Environ. Epidemiol.* **2021**, *5* (5), No. e169, DOI: 10.1097/EE9.0000000000000169.

(41) Huber, V.; Krummenauer, L.; Peña-Ortiz, C.; Lange, S.; Gasparrini, A.; Vicedo-Cabrera, A. M.; Garcia-Herrera, R.; Frieler, K. Temperature-related excess mortality in German cities at 2° C and higher degrees of global warming. *Environ. Res.* **2020**, *186*, No. 109447.

(42) Wang, Y.; Wang, A.; Zhai, J.; Tao, H.; Jiang, T.; Su, B.; Yang, J.; Wang, G.; Liu, Q.; Gao, C. Tens of thousands additional deaths annually in cities of China between 1.5 and 2.0 C warming. *Nat. Commun.* **2019**, *10* (1), No. 3376, DOI: 10.1038/s41467-019-11283-w.

(43) Sun, Z.; Wang, Q.; Chen, C.; Yang, Y.; Yan, M.; Du, H.; Chen, K.; Ji, J. S.; Li, T. Projection of temperature-related excess mortality by integrating population adaptability under changing climate—China, 2050s and 2080s. *China CDC weekly* **2021**, *3* (33), 697−701, DOI: 10.46234/ccdcw2021.174.

(44) Chen, Y.; Guo, F.; Wang, J.; Cai, W.; Wang, C.; Wang, K. Provincial and gridded population projection for China under shared socioeconomic pathways from 2010 to 2100. *Sci. Data* **2020**, *7* (1), No. 83, DOI: 10.1038/s41597-020-0421-y.

(45) Lay, C. R.; Sarofim, M. C.; Zilberg, A. V.; Mills, D. M.; Jones, R. W.; Schwartz, J.; Kinney, P. L. City-level vulnerability to temperature-related mortality in the USA and future projections: a geographically clustered meta-regression. *Lancet Planet. Health* **2021**, *5* (6), e338−e346.

(46) Åström, D. O.; Tornevi, A.; Ebi, K. L.; Rocklöv, J.; Forsberg, B. Evolution of minimum mortality temperature in Stockholm, Sweden, 1901−2009. *Environ. Health Perspect.* **2016**, *124* (6), 740−744.

https://doi.org/10.1021/acs.est.3c09162
Environ. Sci. Technol. XXXX, XXX, XXX−XXX